Significant atmospheric nonlinearities in the ENSO cycle

Sjoukje Philip *
KNMI, De Bilt, The Netherlands

Geert Jan van Oldenborgh
KNMI, De Bilt, The Netherlands

*Corresponding author address: Sjoukje Philip, KNMI, De Bilt, The Netherlands.
E-mail: philip@knmi.nl

Abstract

The nonlinearities that cause El Niño events to deviate more from the mean state than La Niña events are still not completely understood. In this paper we investigate the contribution of one candidate mechanism: ENSO nonlinearities originating from the atmosphere. The initially linear Intermediate Complexity Model of the equatorial Pacific ocean in which all couplings were fitted to observations describes the ENSO cycle reasonably well. In this linear model we systematically introduce extra terms in the atmospheric component. These are the nonlinear response of mean wind stress to SST anomalies, the skewness of the driving noise term in the atmosphere and the relation of this noise term to the background SST or the ENSO phase. The nonlinear response of mean wind stress to SST in the ENSO region is found to be the dominant term influencing the ENSO cycle. However, this influence is only visible when noise fields are used that are fitted to observed patterns of prescribed standard deviation and spatial decorrelation. Standard deviation and skewness of noise do have a dependence on the ENSO phase, but this has a relatively small influence on the ENSO cycle in this model. With these additional nonlinearities in the representation of the atmosphere a step forward has been made towards building a realistic reduced complexity model for ENSO.

1. Introduction

Theoretical explanations for the climate phenomenon El Niño – Southern Oscillation (ENSO) have been developed and models have become more advanced and more reliable. Although El Niño forecasts are reasonably reliable up to about three to nine months ahead (depending on the season), the physical mechanisms determining the onset of an event and nonlinearities in the ENSO phenomenon are not yet well understood. A major nonlinearity is the larger magnitude of the positive sea surface temperature (SST) anomalies, El Niño, compared to the negative SST phase, La Niña. Defined with respect to the mean state, La Niña events occur more frequently than El Niño events but are weaker. The relative importance of the atmospheric contribution to the atmosphere-ocean coupled ENSO cycle for this nonlinear behavior is still a subject of discussion.

Different types of nonlinearities have been discussed in previous studies. Kessler and Kleeman (2000) found evidence that the location of the edge of the warm pool is a measure of the size of the area where Madden-Julian Oscillation (MJO) events occur. Through feedbacks in the ocean and atmosphere oscillating MJO events result in a mean westerly wind, which in turn enlarges the area where the MJO events occur. This strengthens the positive feedback between wind and SST during El Niño, but weakens it during La Niña, giving rise to the observed asymmetry. Jin et al. (2003) claim that nonlinear dynamical heating is an important nonlinearity in the eastern Pacific. During El Niño easterlies in the east Pacific enhance vertical advection of anomalous warm water that accelerates the surface warming, whereas during La Niña westerlies in the east Pacific reduce upwelling and slow down the surface cooling.

Most Intermediate Complexity Models (ICMs) like the Cane-Zebiak model (Zebiak and Cane 1987) have a nonlinearity in the oceanic and/or atmospheric part. In the Cane-Zebiak model, for example, the nonlinearity in the ocean is characterized by a nonlinear coupling between SST and the thermocline depth. This is based on the observation that around the thermocline the temperature is a very nonlinear function of depth. The assumption is then made that raising or lowering the thermocline also has a nonlinear effect on SST. However, such a nonlinear coupling between SST and the thermocline depth is not clearly seen in observations (not shown). Nevertheless, these models describe characteristics of the ENSO cycle like amplitude, frequency and sometimes also skewness in SST better than linear models. Also, there is evidence that nonlinearities in the atmosphere play a role as well, e.g., the wind stress response to SST anomalies is not linear everywhere, and noise components in the wind that drive anomalies in the ocean can depend strongly on the background SST, like in the model of Kleeman et al. (1995). The representations of the atmosphere and atmospheric couplings to SST in ICMs range from totally linear to strongly nonlinear. Often the non-linear component is not as strongly constrained by observations as the dominant linear response.

Most state-of-the-art climate models do not simulate the ENSO skewness correctly. Even if the balance between El Niño and La Niña events is reasonable, the nonlinearities in other aspects differ from observations, casting doubt on the correctness of the representation of the nonlinearities in these models (van Oldenborgh et al. 2005). Therefore, in this study we investigate some nonlinearities in the atmospheric dynamics in observations and re-analyses.

One of the most obvious nonlinearities in the atmospheric dynamics is the difference in response of wind stress to positive or negative SST anomalies. Here we can distinguish between the mean response of wind stress to SST and higher moments that characterize the atmospheric noise driving the ocean dynamics. Previous studies have approached these nonlinearities in the atmospheric dynamics in several ways. Sura et al. (2005) already demonstrated that a simple

linear system with multiplicative noise (i.e., noise with an amplitude depending on the background state) can result in a non-Gaussian distribution. The application can be found in Sura et al. (2006), who is show that for mid-latitude SST anomalies inclusion of a multiplicative noise term does result in skewed SST. The net effect of multiplicative noise is thus a nonlinear response of the atmosphere. Therefore throughout this article multiplicative noise is ranged among nonlinear effects.

Perez et al. (2005) studied the difference between the influence of additive and multiplicative noise in the atmosphere driving the ocean on the ENSO probability density function. For the additive noise they used 25 empirical orthogonal functions (EOFs) of noise in the wind stress component with a stochastic forcing amplitude that is a linear function of the Niño3 index (5°S–5°N, 150°W–90°W). They show that the dynamics of the system are different for additive and multiplicative stochastic forcing and additive forcing alone does not reproduce the variability well. Eisenman et al. (2005) use westerly wind events (WWEs) with fixed spatial structure and duration. They show that the influence of WWEs is enhanced when the occurrence of WWEs is no longer only additive but has a deterministic part which is purely a function of the warmpool extend. The modulation of the occurrence of WWEs by the large-scale equatorial SST field enhances the low frequency component of WWEs. The mechanism behind this is that for higher SSTs more WWEs can occur and accumulation of these WWEs can induce a warming event. The effect of migration of WWEs with the warmpool (Gebbie et al. 2006) is shown to be important for ENSO dynamics, where eastward migration and modulation of WWEs during a warm event enhance the amplitude of ENSO. Tziperman and Yu (2007) discuss a parameterization of the nonlinear modulation of pattern, amplitude and timing of WWEs by SST. They find that WWEs are not totally additive but partly multiplicative since ENSO and the seasonal cycle dominate the characteristics of the WWEs. Lengaigne et al. (2004) made an analysis of WWEs in a coupled general circulation model. They show that the coupled response is strongly sensitive to WWEs and one of the responses to a WWE is an eastward displacement of the warmpool.

In this study we want to investigate the influence of nonlinearities that are fitted to observations of the ENSO cycle. For this, we take the opposite approach to studies that start from a model and tune nonlinear properties of the atmosphere such that the model output resembles observations the best. We first deduce the nonlinear properties of the atmosphere from observations, and next use a tuned reduced model to investigate the effects of each nonlinear term on the ENSO cycle. The starting point of the study is the ICM consisting of the linear feedbacks studied in van Oldenborgh et al. (2005), completed with a linear ocean model (Burgers et al. 2002). In this model, noise is represented in the form of Gaussian perturbations of the wind patterns corresponding to the Niño3 and Niño4 indices, taking into account the correlation between the Niño3 and Niño4 indices and the temporal correlation of the observed wind patterns (Burgers and van Oldenborgh 2003). This model performs reasonably well with only linear dynamics but nonlinearities in the ENSO cycle are obviously not represented. In our study some nonlinearities are added in order to build a more realistic ICM and obtain more insight in the dynamics of ENSO.

In this paper the atmosphere is represented by a statistical model of wind stress that consists of a combination of a deterministic and a stochastic term. The deterministic term can be either a linear or nonlinear function of SST anomalies. The stochastic term is defined in terms of the standard deviation and skewness of noise, each of which are two-dimensional functions of SST, and have realistically prescribed spatial and time correlations. For both deterministic and noise

wind stress terms, the functional relationships to SST anomalies are found empirically. Using this model the following terms that lead to a nonlinear model are studied:

1. the dependence of the mean westerly wind anomaly on background SST; in practice this can be done by investigating the nonlinear response of wind stress to SST.

2. the standard deviation and skewness of the atmospheric noise distribution.

3. the relation between this noise distribution and background SST.

The questions addressed in this paper are: does an ICM with coupling parameters fitted to observations describe the ENSO cycle well, including nonlinearities? And which of the nonlinear aspects of the atmosphere mentioned above is most important in generating the skewness in SST in the ENSO cycle?

The methodology of this study and the model are described in Section 2. In Section 3 we describe the different characteristics of the atmospheric noise. Implications of these characteristics for the ENSO cycle are shown in Section 4. Finally we discuss the results and conclude in Section 5.

2. Method of investigation

In Figure 1 a conceptual model of ENSO is shown, with feedbacks between zonal wind stress (τ_x), SST and thermocline depth (Z_{20}). The ICM that is built from this conceptual model is based on the so called Gmodel (Burgers et al. 2002; Burgers and van Oldenborgh 2003). The linear couplings between SST and wind stress, and the dependence of SST on thermocline depth (Figure 1a) were investigated in detail by van Oldenborgh et al. (2005). In order to complete the reduced model, the different descriptions of the driving external atmospheric noise term and the internal nonlinear response of wind stress to SST are investigated (Figure 1b). The findings are added one by one to the originally linear reduced model and the ENSO properties in the complete reduced model are studied.

The description of the model is organized as follows. Details of the statistical atmosphere are given in Section 2a. Characteristics of the external noise term are discussed in Section 2b-c. Furthermore, the ocean model is described in more detail in Section 2d and the data and different types of model experiments are discussed in Section 2e.

a. Statistical atmosphere: mean response to background SST

The atmosphere is described by a statistical atmosphere model where local SST anomalies result in zonal wind stress patterns, as the most important atmospheric forcing is the zonal wind stress component. Nonlinearities are added to a linear statistical description of the atmosphere.

Our starting point is a linear statistical atmosphere model where wind stress anomalies are described as a direct response to SST anomalies in separate regions near the equator:

$$\tau_x'(x,y,t) = \sum_{i=1}^{n} A_1(x,y)_i T_i'(t) + \epsilon_1(x,y,t) \tag{1}$$

where $\tau_x'(x,y,t)$ is the zonal wind stress anomaly and $T_i'(t)$ are SST anomalies averaged over standard regions. $A_1(x,y)_i$ are the domain-wide wind stress patterns corresponding to the SST anomalies of the separate regions $i = 1, 2, ..., n$. The term $\epsilon_1(x,y,t)$ denotes the stochastic

forcing by random wind stress variations. In the Gmodel this is not white noise, as the wind varies only on weekly time scales. As the model is integrated in time steps of 8 hours, the forcing varies slowly compared to other processes and the equations can be solved using the normal method for equations with additive noise.

In this study, SST variations are summarized as the average temperature anomalies in 2 equal-sized boxes (more boxes would give too much noise) along the equator in 5°S–5°N, 160°E–90°W. With this choice $T_i'(t)$ corresponds approximately to the Niño-indices, with $T_1'(t) \approx$ Niño4 and $T_2'(t) \approx$ Niño3. The motivation for this choice will be explained in Section 3. The effects of temperature anomalies in the two boxes on wind stress are investigated separately. For the linear statistical atmosphere model this is mathematically equivalent to dividing the regression of wind stress on the Niño-indices by the covariance matrix of the Niño-indices: the two wind stress patterns then correspond to an SST anomaly in one of these two boxes only and not to anomalies in the other box.

A nonlinear version of the statistical atmosphere has been constructed by including the next term in a Taylor expansion:

$$\tau_x'(x,y,t) = \sum_{i=1}^{n} A_2(x,y)_i T_i'(t) + \sum_{j=1}^{m} B(x,y)_j T_j'^2(t) + \epsilon_2(x,y,t) \tag{2}$$

where $A_2(x,y)_i$ and $B(x,y)_j$ are domain wide wind stress patterns corresponding to the linear and squared SST anomalies $T_i'(t)$ respectively. The number of boxes n and m and the domains do not have to be identical, and in this study the linear part is defined as in Equation 1, whereas for the nonlinear part we use $m = 1$ over the area 5°S–5°N, 145°W–118°W. This is approximately the western half of Niño3. The motivation for this choice will be explained in Section 3a. The nonlinear part can be seen as the integrated effect of the nonlinear dependence of the mean wind stress to SST anomalies, resulting in an extra mean westerly wind anomaly during both warm and cold events.

In the experiments where we use the nonlinear statistical atmosphere, the quadratic term in the atmosphere is the only nonlinear term in the model. Since in the ICM this term is never compensated by nonlinear damping terms, we cut off the nonlinear statistical atmosphere term at an SST anomaly index of $\pm 2K$, which is corresponds to a fairly strong El Niño/La Niña. Results are qualitatively robust when we vary the cut off around this value of $\pm 2K$.

The wind stress patterns for observational data $A_2(x,y)_i$ and $B(x,y)_i$ are shown in Section 3a.

b. Statistical atmosphere: characteristics of noise

An observed atmospheric noise is constructed by subtracting the wind stress calculated with Equation 1 or 2 from the total observed wind stress. These residuals force the ENSO oscillations in this (intrinsically stable) noise-driven ENSO model. The timescale on which the stochastic noise terms vary (1 week) is much longer than the integration time-step of the Gmodel (1/3 day). The characteristics of noise can be described in several ways, ranging from quite simple to more advanced descriptions. In this study the noise terms are characterized with statistical parameters.

In the original, linear version of the Gmodel red plus white noise has been added to the Niño-indices instead of adding the full noise field to the wind stress. The use of red and white noise appears a better approximation for the autocorrelation of the residuals than only adding white noise (Burgers and van Oldenborgh 2003). Effectively, this relatively simple description

of noise is a method to simulate the effect of perturbations of the coherent wind fields associated with the Niño-indices. The effect of this parameterization of the noise on the ENSO cycle is very similar to that of the full noise field in terms of wind stress (Burgers and van Oldenborgh 2003). However, in this study we aim to get more insight in the details and nonlinearities of the full noise field. A better parameterization of the spatial variability of the noise field on smaller scales over the whole equatorial Pacific is then needed. Rather than applying noise to the Niño-indices, we explicitly describe the full noise field in terms of a larger number of two-dimensional parameters.

One possibility to describe the full noise field is by using EOFs (Perez et al. 2005). We did not use this approach, where the standard deviation and skewness of this EOF-based noise field can not easily be brought in agreement with observations. Moreover, patterns of the first few noise-EOFs give rise to spurious long-distance correlations. These correlations give undesirable effects on the ENSO cycle in the ICM. To avoid this effect we try a method in which the noise standard deviation, skewness and spatial and temporal correlation are preserved.

In this study another method has been used, in which the noise has been modeled as a stochastic field with spatially prescribed standard deviation, prescribed spatial correlations and time correlation and optionally spatially prescribed skewness in the equatorial Pacific basin. The statistical parameters of the stochastic field are derived from the observed noise fields. The observed fields are described in Section 3e. From these noise fields the 2-dimensional fields for standard deviation and skewness are calculated. These fields are shown in Section 3b. The spatial autocorrelation length is described well by a constant 36 degrees in latitude and 6-8 degrees in longitude. The time correlation is fitted from the weekly observed noise and varies from 0.9 near the equator to almost zero at the northern and southern edges of the domain. For more details see Appendix A.

Ronstructed fields with these three or four characteristics (without or with prescribed skewness) are used as noise fields. Technically, this noise field is implemented by a diffusion operator. This operator generates a spatially correlated field from an uncorrelated noise field that is drawn randomly from a normal distribution with prescribed standard deviation over the whole basin. Optionally, for a non-zero skewness the field is then distorted to the observed skewness. For details of the implementation, see Appendix B.

c. Dependence of noise characteristics on the ENSO cycle

In order to complete the description of noise characteristics and their dependence on the ENSO cycle, the relationship between the standard deviation and skewness of the noise and the ENSO phase has been investigated. Note that the dependence of the mean wind stress response on the ENSO phase is described by the nonlinear statistical atmosphere. Concerning the standard deviation and skewness, the timeseries of the noise is split into three categories depending on the ENSO phase. These three ENSO phases are defined as high, normal or low SST in the central box (El Niño, neutral or La Niña), where all three categories are equally likely by definition. Then, for each of these three phases the standard deviation and skewness fields are computed separately. The implementation of the noise fields in the reduced ENSO model is the same as described in the previous section, except that the parameters are selected on the basis of the category in which the SST anomaly falls: positive, neutral or negative.

d. Ocean model

Simulations are performed with the so-called Gmodel, an equatorial Pacific coupled ICM. This model consists of a linear 1.5-layer reduced-gravity ocean model, a linear statistical atmosphere and a linear SST anomaly equation (Burgers et al. 2002; Burgers and van Oldenborgh 2003). The model domain ranges from 30°S to 30°N and 122°E to 72°W, on a $2^\circ \times 1^\circ$ longitude-latitude grid with realistic coast lines. The ocean model solves the shallow water equations (Gill 1982). A Kelvin wave speed is fitted for the best ocean dynamics in the un-coupled version of the model: a value of 2.5 m/s is used in the ocean model.

In addition to the linear 1.5-layer reduced-gravity ocean model, a linear SST anomaly equation is used, as shown in Figure 1. This SST equation for the ocean model describes the SST response to thermocline anomalies Z'_{20}, the SST response to wind variability and damping on SST anomalies T'. In the local SST equation:

$$\begin{aligned} \frac{dT'}{dt}(x,y,t) &= \alpha(x,y)\, Z'_{20}(x,y,t-\delta) + \\ &+ \beta(x,y)\, \tau'_x(x,y,t) - \gamma(x,y)\, T'(x,y,t), \end{aligned} \tag{3}$$

the SST response to thermocline anomalies α, the SST response to wind variability β and the damping term γ are fitted to monthly SODA ocean re-analysis data (Carton and Giese 2006). van Oldenborgh et al. (2005) give a more detailed description of the SST equation parameters. These parameters are 2-dimensional fields, but since sufficient observations are only available between 8°S - 8°N, outside this region values of the parameters are tapered off to very small values for α and β and to intermediate values for γ. The 2-dimensional fitted parameters deduced from SODA data and used in the Gmodel are shown in Figure 2. SST variability caused by thermocline anomalies (α) is strongest in the east Pacific where the thermocline is shallowest. The response of SST to wind stress anomalies (β) plays a role in SST variability in both the eastern and central Pacific. However, the wind stress variability in the eastern Pacific is much smaller, so this term is most important in the central Pacific. The absolute damping (γ) is strongest in the east Pacific, but compared to the other terms damping is very large in the West Pacific. This is likely an effect of the cloud feedback that is strongest over the warmer West Pacific where cloud formation takes place (Philip and van Oldenborgh 2006).

e. Data and experiments

The ocean parameters are fitted to the monthly SODA 1.4.2/3 0.5° ocean re-analysis dataset (Carton and Giese 2006), which is a mixture between observations and model calculations.

For the statistical atmosphere, weekly ERA40 data (Uppala et al. 2005) have been used. With 45 years of weekly ERA40 data the linear response to SST anomalies in 2 boxes in the Pacific Ocean can be resolved. Using more, smaller, boxes gives rise to too much noise in the response patterns. Since each of the boxes cover more than one third of the zonal extend, the longitudinal extent of these two boxes is quite large compared to the equatorial Pacific ocean.

The ICM is driven by atmospheric noise as described above. In the context of this model, the effects of the nonlinearities have been investigated in isolation and together, keeping the modeled dynamics of the ocean linear. In Table 1 the different types of ICM experiments are listed with their abbreviations used throughout the text. The first category of experiments differs in the linear or nonlinear statistical atmosphere; *lin*- and *nonlin*-experiments. The second category distinguishes between relatively simple noise on the Niño-indices or a distribution of

spatial noise fields on the wind stress, either characterized by standard deviation or by standard deviation and skewness; *nino-*, *full-sd-* and *full-skew*-experiments. In the last category the full noise fields can be chosen to be dependent or independent on the phase of the ENSO cycle; *fix*- and *phase*-experiments. For readability in the rest of this paper the three types of noise will be referred to as 'nino noise', 'full sd noise' and 'full skewed noise'. All combinations have been explored but in this paper only the most interesting results are discussed in detail. The model run length for every experiment is 400 years, so that we have a balance between statistical errors and run time. The most important ENSO parameters that can change in the ICM by adding different types of noise are the first EOF, the period and skewness of SST. These diagnostics from the ICM output are compared with observations.

3. Atmospheric ENSO response and noise

The standard Gmodel experiment with ocean parameters and a linear statistical atmosphere fitted to observations (*lin/nino/fix*) is driven by noise that has a relatively simple description, i.e. red and white noise on the Niño-indices. The linear relationship between SST and deterministic wind stress for the two boxes ($A_2(x,y)_i$ in Equation 2 with $i = 1, 2$) is shown in Figure 3a-b. The linear response $A_1(x,y)_i$ in Equation 1 differs only slightly from the first order term $A_2(x,y)_i$ and is not shown. The patterns resemble somewhat a Gill-type pattern (Gill 1980), but differ in many details such as the relative strengths of the equatorial poles and the off-equatorial structure (see also van Oldenborgh et al. 2005). The linear wind response to a positive SST anomaly in the western box is directed eastward in the western Pacific and westward in the east Pacific. The wind response to a positive SST anomaly in the eastern box is eastward in the central Pacific.

The response to an SST anomaly in the western Pacific is stronger than the response to the same anomaly in the eastern Pacific. This is caused by the non-linear response of convection to SST depending on he background temperature (e.g., Philip and van Oldenborgh 2006). Over high SST a small SST anomaly gives a larger latent heat release than the same SST anomaly over lower SST. The wind stress response is proportional to the heat source, hence it is stronger in the western Pacific.

The wind stress patterns of the statistical atmosphere in the Pacific Ocean are relatively stationary and not sensitive to the exact location and size of the boxes. If for instance two equal sized boxes between 180°E–80°W instead of 160°E–90°W are used the overall wind stress patterns are located at the same position (not shown, see also van Oldenborgh et al. 2005). The standard deviation of the remaining noise fields is somewhat lower for the Niño-based atmosphere than for the atmosphere based on the alternative boxes mentioned before. Therefore it is reasonable to use the statistical atmosphere based on approximately the standard Niño-indices.

In the next subsections the noise component and statistical atmosphere as derived from observations are discussed in detail.

a. Nonlinear atmospheric response

Figure 3c shows the observed second order term of the statistical atmosphere in the box that selects the western half of the Niño3 region, i.e. the quadratic response to an SST anomaly $B(x,y)_1$ in Equation 2. Like the linear wind stress response, the pattern of the nonlinear wind stress response is quite stationary and most of the variance of the noise that can be described by

quadratic terms is explained by adding only this box. It shows a positive, eastward response of the wind to both positive and negative SST anomalies, with a maximum situated at the edge of the warm pool. This implies that the average westerly (eastward) wind response in the central Pacific during El Niño is larger than the easterly (westward) response to an equal-strength La Niña. This can be understood in terms of the background SST, with a larger effect of convective activity over a larger warm pool area during El Niño. Whereas the linear wind response to SST anomalies assumes a constant background SST, the nonlinear response shows the effect of the change in background SST, especially at the edge of the warm pool. During El Niño the convection zone is enlarged and the response is enhanced. Since the response is positive, this results in an enhancement of the westerly anomalies during El Niño. On the other hand, during La Niña the convection zone is reduced and the response is lower. Since the response during La Niña is negative the net effect is again positive.

Kessler and Kleeman (2000) already showed this phenomenon in a much simpler model, where wind stress similar to that of the Madden-Julian Oscillation develops a rectified SST anomaly additional to the linear response. This leads to cooling in the West Pacific and warming in the East Pacific. In other words, the zonal gradient is smaller and therefore more westerly winds can occur, resulting in a mean westerly wind. The result is confirmed by Lengaigne et al. (2003) who show in an atmospheric general circulation model that the eastward displacement of the warmpool induces an eastward shift of convection, which in turn promotes the occurrence of WWEs. The additional WWEs result in a net westerly response.

b. The full noise field

The noise field of observational data can be calculated either based on the linear statistical atmosphere (Equation 1, not shown), or based on the nonlinear statistical atmosphere (Equation 2). From the noise field the standard deviation and skewness are determined. The fields corresponding to the nonlinear statistical atmosphere are shown in Figure 4. The figures corresponding to the linear statistical atmosphere are qualitatively the same.

Standard errors Δ in standard deviation σ and skewness η are approximated with $\Delta_\sigma = \sigma/\sqrt{2N}$ and $\Delta_\eta = \sqrt{6/N}$ respectively, where N is the number of independent values. As we use 45 years of observations and 400 years of model data and using a temporal decorrelation length of 4 weeks for noise and 6 months for SST the numbers of independent values become: $N_{\mathrm{noise-observed}} = 540$, $N_{\mathrm{noise-Gmodel}} = 2400$, $N_{\mathrm{SST-observed}} = 90$ and $N_{\mathrm{SST-Gmodel}} = 400$. This gives a standard error of 0.03σ for the standard deviation and 0.11 for the skewness in the observational noise fields.

As can be seen in Figure 4 the noise amplitude is lowest in the eastern equatorial region where the background SST (not shown) is lowest. Furthermore, the skewness shown in Figure 4 reflects stronger westerly wind anomalies than easterly wind anomalies in the West Pacific. This describes the fact that WWEs are westerly, not easterly. The region of the highest skewness is located slightly south of the equator, which is in accordance with the location of the highest climatological SST (not shown).

The driving noise fields are constructed as described in Section 2b and Appendix A and B, with standard deviation (and optionally skewness), and spatial and temporal decorrelation scales prescribed from observations. We checked that the constructed noise field reproduces the standard deviation of the observed noise quite well. The skewness is reproduced by definition.

c. ENSO-phase dependent noise

First we show that the standard deviation and skewness of the observed noise depends on the ENSO-phase. The noise standard deviation and skewness of the warm- and cold-SST phases ($\sigma_{\mathrm{warm}}, \sigma_{\mathrm{cold}}, S_{\mathrm{warm}}$ and S_{cold}) are compared to noise standard deviation and skewness of the neutral phase ($\sigma_{\mathrm{neutral}}$ and S_{neutral}). Figure 5 shows the differences of the standard deviation as $(\sigma_{\mathrm{warm}} - \sigma_{\mathrm{neutral}})/(\sigma_{\mathrm{warm}} + \sigma_{\mathrm{neutral}})$ and $(\sigma_{\mathrm{cold}} - \sigma_{\mathrm{neutral}})(\sigma_{\mathrm{cold}} + \sigma_{\mathrm{neutral}})$. A value of 0.1 thus means an increase in standard deviation of 22%, a value of -0.1 means a decrease of 18%. White areas mark non-significant changes with respect to the neutral phase. One can see that not only the mean westerly wind stress increases during El Niño, as shown in Section 3a, but also the amplitude of the noise becomes stronger for higher temperatures. The standard deviation of the noise in the El Niño phase is up to 35% higher than for neutral temperatures, especially in the West Pacific where the standard deviation is already higher than in the east equatorial Pacific. On the other hand, for La Niña the amplitude is up to 25% weaker.

Figure 6 shows the skewness of noise for the warm, neutral and cold SST ENSO phases. During El Niño significant changes can be found in the central Pacific: westerlies are spread out over a larger area since the area of the warm pool is extended. During La Niña a significant reduction in skewness of the noise is seen in the West Pacific. The higher skewness in the west equatorial Pacific during neutral conditions than El Niño conditions is statistically significant. This is in agreement with Monahan (2008) who shows that the skewness of zonal wind stress is highest for intermediate values of the ratio of the mean and the standard deviation of zonal wind stress. In an idealized stochastic boundary layer model he demonstrates that the skewness is determined by both the nonlinearity of the relationship between winds and wind stresses and the non-Gaussianity of the vector winds.

4. Implications for the ENSO cycle

In Figure 7 the first EOF, spectrum of the corresponding principal component (PC1) (which indicates the period of the ENSO cycle) and skewness of SST of the linear ICM *lin/nino/fix*-experiment are shown and compared to observations. Standard errors are 0.26 in the observed skewness of SST and 0.12 for the ICM SST skewness. In addition to the significance level of the spectrum, there is an error in the power of the spectrum due to sampling (not shown). Comparing the spectra of different Gmodel runs to each other it appears that the widths of the spectra are robust, but single peaks cannot be interpreted in terms of dynamics.

The maximum of the first EOF of the *lin/nino/fix*-experiment is too far west, the period is too frequent and slightly peaked around 3 years and the skewness of this ICM is, as expected for a linear model, not discernible from sampling noise.

Overall, this ICM output is encouraging since the components of the ENSO cycle seem modelled well enough to approximate the main properties of ENSO. However, a better description of the driving noise component and the statistical atmosphere are required in order to improve the first EOF, the spectrum and the skewness of SST.

Figures 8-10 show the most important implications of the nonlinear features discussed in this study for the ENSO cycle simulated by the ICM with nonlinear effects in the atmosphere added one by one.

Considering the first EOF of the ICM, adding a spatially distributed noise field on the wind stress field has the largest influence compared to the standard experiment (*lin/nino/fix*). With the use of 'full sd noise' or 'full skewed noise' (all *full-sd-* and *full-skew-* experiments) the first

EOF is strongly improved with respect to the *lin/nino/fix*-experiment. With a full noise field the maximum of the first EOF is no longer too far west. Although the pattern is spread out somewhat more westward than in the observations, it is in good agreement with the first EOF of observed SST. The result for the *lin/full-sd/fix*-experiment is shown in Figure 8. The EOFs for the other experiments are not shown, since differences of the first EOF between the *lin*- and *nonlin*-experiments and *fix*- and *phase*-experiments are much smaller than the difference between experiments with 'nino noise' and experiments with 'full sd noise'.

Next, the power spectrum of PC1 is investigated, see Figure 9. The period is affected most by adding 'full sd noise' to the ICM and by using the quadratic term in the atmosphere, and by the combination of the two. The influence of 'full skewed noise' and ENSO phase dependent noise is much smaller and results are not shown. For all experiments with a spatially distributed noise field the power spectrum has become a little broader. For all *nonlin/full*-experiments the maximum around 3 years is broadened and shifted to around 4 years.

Finally, the SST skewness of the ICM simulations is considered. SST skewnesses of a selection of experiments are shown in Figure 10. The simulations with linear statistical atmosphere show very low or even no significant SST skewness: the *lin/full-sd/fix*-experiment exhibits no significant SST skewness and the *lin/full-sd/phase*-experiment has a small signal in the west Pacific. Changing the noise field into a full skewed noise field results in a small SST skewness in the West Pacific. The effect of the use of the nonlinear statistical atmosphere is much larger, especially in combination with a full noise field. The SST of the ICM simulations is much more positively skewed, albeit only in the Central Pacific. Whereas the *nonlin/nino/fix*-experiment still shows only a small (significant) skewness, the SST of other *nonlin*-experiments turn out to be strongly skewed with skewnesses exeeding 1. The impact of using the nonlinear statistical atmosphere in combination with a 'full sd noise' field is very distinct. On the contrary, with phase-dependent noise or 'full skewed noise' SST skewness in the ICM shows only little changes. Therefore only the *nonlin/full-sd/fix*-experiment is shown.

Overall, it seems to be necessary to use full noise fields with spatially varying standard deviation instead of simple noise terms on the SST indices in order to obtain more realistic ENSO characteristics like the first EOF and spectrum. However, using 'full sd noise', the nonlinearities in SST are seen to be dominated by the nonlinear statistical atmosphere, i.e. the nonlinear mean westerly wind response to SST in the ENSO region. This means that the integrated effect of the enhanced westerly wind events over the larger warm pool has a dominant influence on the difference in strength of El Niño relative to La Niña; other atmospheric aspects such as the skewness of the full noise fields are less important. Making the standard deviation (and alternatively skewness as well) of the noise dependent on the ENSO phase does not influence either the ENSO cycle nor the skewness of SST strongly in our modelling approach.

5. Conclusions and discussion

The purpose of this investigation was to quantify the role of nonlinearities in the atmospheric components of the ENSO cycle. This was studied in a reduced model containing the most important dynamics of the ENSO cycle, the components of which are fitted separately to observations. The linear starting point describes the ENSO cycle reasonably well. One of the most obvious problems in this model is the absence of nonlinearities. The most distinct is the skewness of SST: in reality El Niño events are in general stronger than La Niña events. Nonlinearities in atmospheric responses and in the driving noise terms with characteristics close to

observed atmospheric nonlinearities are added.

Adding the fitted nonlinearities in the atmosphere, the output of the ICM indicates that the nonlinear mean response of wind stress to SST in the ENSO region has a dominant influence on the nonlinearities in SST in the ENSO cycle. However, the use of spatial noise fields with standard deviation, spatial decorrelation and temporal decorrelation similar to observed ('full sd noise') is necessary for a better description of characteristics like the first EOF and spectrum. With this description of the noise fields the first EOF is no longer too far to the central Pacific but located more in the east Pacific, as consistent with observations. The effects of using ENSO phase dependent (multiplicative) noise are relatively small. The skewness of the full noise fields (i.e. westerly wind events rather than symmetric or easterly ones) also has a minor effect.

In the investigation of the influence of atmospheric noise like WWEs on the nonlinearities in the ENSO cycle a distinction can be made between different aspects of WWEs. These can be expanded into mean, variance and skewness. In most studies where multiplicative noise is used in addition to stochastic noise (e.g., Perez et al. 2005; Eisenman et al. 2005; Gebbie et al. 2006; Tziperman and Yu 2007) the focus is on the ENSO-phase dependent variance of WWEs. In this study we show that the mean effect of WWEs is much more important for ENSO skewness than the variance. Furthermore, this study shows that both the skewness of noise fields (i.e. westerly wind events) and the multiplicative nature of the noise influence SST skewness less.

Kessler and Kleeman (2000) already showed that the wind stress similar to that of the Madden-Julian Oscillation develops a rectified SST anomaly, which in turn results in a positively skewed SST. The MJO patterns used by Kessler and Kleeman (2000) are idealized sinusoidal waves in x and t. In this study the result is more general than that of Kessler and Kleeman (2000), since asymmetric WWEs can occur as well and the amplitude of WWEs can become larger. The main result is confirmed, i.e. the nonlinear relation between SST and wind stress is responsible for a skewed SST signal. This study furthermore shows that this is the most significant atmospheric contribution to SST skewness, more important than the contributions of the relation of amplitude and skewness of atmospheric noise to the background SST.

The atmospheric properties discussed so far have large implications for the modeled SST skewness. However, the skewness is still too strong in the central Pacific and too weak in the east Pacific. This is partly due to the ocean part of the ICM that is totally linear in the version of the ICM used so far. Note that so far no seasonal cycle is included in the ICM.

An improvement of the description of nonlinearities in the ocean part in the ENSO feedback will be needed. This study is concerned with the nonlinearities that arise from the atmosphere only. Preliminary results indicate that adding nonlinearities in the ocean model improves the skewness. Adding the restriction that the thermocline cannot outcrop above the sea surface improves the simulation of the skewness in both the central and east Pacific, see Figure 10f.

In addition, in the central Pacific, the relation between wind stress and local SST in observational data shows indications for nonlinearities. During El Niño the anomalous zonal ocean velocity u' is positive. At the same time, in general the zonal temperature gradient T'_x becomes less negative, so it has a positive anomaly. During La Niña these anomalies change sign. Thus, the second order anomalous term $u'T'_x$ tends to be positive during both warm and cold events. This results in an enhancement of La Niña and a weakening of El Niño, which in turn influences the skewness of SST in this region. The result is a shift towards lower skewness. In the east Pacific other nonlinearities in the ocean are important, see among others Zebiak and Cane (1987) and Jin et al. (2003). We expect that the inclusion of the most important oceanic nonlinearities to extend the reduced model will give a good description of the complete ENSO cycle.

Acknowledgments.

We kindly thank Bart van den Hurk for comments and suggestions. This manuscript has improved by the comments of two anonymous reviewers. ERA-40 data have been obtained from the ECMWF data server. This research is supported by the Research Council for Earth and Life Sciences (ALW) of the Netherlands Organisation for Scientific Research (NWO).

APPENDIX A

Spatial and Time Correlations of the Noise

Results in this study are not very sensitive to the exact numbers of the spatial and time-correlations of the noise field but an estimate is needed for the implementation of the noise field in the Gmodel. The spatial and time-correlation are estimated from 25 equally distributed locations between 30°S-30°N, 120°E-270°E, that is, 5 locations zonally times 5 locations meridionally. This number of locations was enough to cover the whole basin. From these locations the spatial correlation of the noise has been calculated to be 36 degrees in longitude (a_x) and 6 (between 10°N and 10°S) to 8 (higher latitudes) degrees in latitude (a_y).

A good approximation of the time-correlation coefficient at lag 1 time unit (one model week) $a_1(x, y)$ is given by a function that varies linearly along the equator and exponentially along the meridionals as $a_1(x, y) = 1.1(1 + x/8N_x)/\exp(\frac{1}{6}|y - \frac{1}{2} - \frac{1}{2}N_y|)$ with x,y ranging from 1 to N_x and 1 to N_y respectively and N_x=84, N_y=30. This gives correlations around 0.9 near the equator and 0.1 near the northern and southern edges of the domain.

APPENDIX B

Reconstruction of Noise Fields

The noise fields used for input in the ICM should have the same standard deviation, skewness and correlations as the original noise field described in Appendix A. This is obtained in four successive steps, with $N_1(x,y,t)$, $N_2(x,y,t)$ and $N_3(x,y,t)$ as intermediate steps.

1. Standard deviation: Gaussian distributed random numbers $\varepsilon(x,y)$, with x and y varying along the domain, are multiplied by the standard deviation of the original noise field $\sigma(x,y)$:
$$N_1(x,y,t) = \varepsilon(x,y)\sigma(x,y) \tag{B1}$$

2. Spatial correlation lengths a_x and a_y: the field obtained by Equation B1 has to be convolved with a two-dimensional normal distribution with prescribed spatial correlation lengths (a_x and a_y) in order to get a noise field with desired spatial correlations:
$$N_2(x,y,t) \sim a_x a_y \int dx'dy' N_1(x',y',t) e^{-\frac{(x-x')^2}{2a_x^2} - \frac{(y-y')^2}{2a_y^2}} \tag{B2}$$
In practice, a diffusion operator is used for the convolution. The diffusion operator is designed to ensure that the standard deviation of $N_2(x,y,t)$ is approximately the same as the original one (Bonekamp et al. 2001).

3. Time correlation $(a_1(x,y))$: the time-correlation with lag 1 is imposed by applying:
$$N_3(x,y,t) = \frac{a_1(x,y)N_2(x,y,t-1) + N_2(x,y,t)}{\sqrt{a_1(x,y)^2+1}} \tag{B3}$$
Note that the standard deviation is still $\sigma'(x,y)$

4. Skewness ($S(x,y)$): in order to preserve the standard deviation $\sigma'(x,y)$ but additionally obtain the desired skewness $S(x,y)$, we solve the equation
$$\begin{aligned} \epsilon(x,y,t) &= A(x,y) + B(x,y)\ N_3(x,y,t) + \\ &+ C(x,y)\ S(x,y)\ N_3(x,y,t)^2 \end{aligned} \tag{B4}$$
for the constants A(x,y), B(x,y) and C(x,y) so that for every location the time mean of $\epsilon(x,y,t)$ is zero, the standard deviation of $\epsilon(x,y,t)$ is $\sigma'(x,y)$ and the skewness of $\epsilon(x,y,t)$ is $S(x,y)$. The solution for $S(x,y) < \sqrt{8}$ is (derivation not shown):
$A(x,y) = -C(x,y)\sigma(x,y)^2 S(x,y)$
$B(x,y) = \sqrt{\cos(2\phi/3) + \sqrt{3}\sin(2\phi/3) - 1}$
$C(x,y) = \dfrac{-\cos(\phi/3) + \sqrt{3}\sin(\phi/3)}{\sqrt{2}\sigma(x,y)S(x,y)}$
with $\phi = -\arctan\left(\sqrt{8 - S(x,y)^2}/S(x,y)\right)$
With this equation the noise field is then transformed towards correct skewness.

These 4 steps are repeated every time that the wind stress field in the ICM is calculated.
The resulting fields are added as driving noise terms to the Gmodel.

References

Bonekamp, H., G. J. van Oldenborgh, and G. Burgers, 2001: Variational assimilation of TAO and XBT data in the HOPE OGCM, adjusting the surface fluxes in the tropical ocean. *J. Geophys. Res.*, **C106**, 16693–16709.

Burgers, G., M. A. Balmaseda, F. C. Vossepoel, G. J. van Oldenborgh, and P. J. van Leeuwen, 2002: Balanced ocean-data assimilation near the equator. *J. Phys. Oceanogr.*, **32**, 2509–2529.

Burgers, G. J. H. and G. J. van Oldenborgh, 2003: On the impact of local feedbacks in the Central Pacific on the ENSO cycle. *J. Climate*, **16**, 2396–2407.

Carton, J. A. and B. S. Giese, 2008: SODA: A reanalysis of ocean climate. *MWR*, **139**, 2999–3017.

Eisenman, I., L. Yu, and E. Tziperman, 2005: Westerly wind bursts: ENSO's tail rather than the dog? *J. Climate*, **18**, 5224–5238.

Gebbie, G., I. Eisenman, A. Wittenberg, and E. Tziperman, 2006: Westerly wind burst modulation by sea surface temperature as an intrinsic part of ENSO dynamics. *J. Atmos. Sci.*.

Gill, A. E., 1980: Some simple solutions for heat induced tropical circulation. *Quart. J. Roy. Meteor. Soc.*, **106**, 447–462.

— 1982: *Atmosphere–Ocean Dynamics*. Academic Press, Orlando, 662 pp.

Jin, F.-F., S.-I. An, A. Timmermann, and J. Zhao, 2003: Strong El Niño events and nonlinear dynamical heating. *Geophys. Res. Lett.*, **30**, 1120, doi:10.1029/2002GL016356.

Kessler, W. and R. Kleeman, 2000: Rectification of the Madden-Julian oscillation into the ENSO cycle. *J. Climate*, **13**, 3560–3575.

Kleeman, R., A. Moore, and N. R. Smith, 1995: Assimilation of subsurface thermal data into a simple ocean model for the initialization of an intermediate tropical coupled ocean–atmosphere forecast model. *Mon. Wea. Rev.*, **123**, 3103–3114.

Lengaigne, M., J.-P. Boulanger, C. Menkes, G. Madec, P. Delecluse, E. Guilyardi, and J. Slingo, 2003: The march 1997 westerly wind event and the onset of the 1997/98 El Niño: Understanding the role of the atmospheric response. *J. Climate*, **16**, 3330–3343.

Lengaigne, M., E. Guilyardi, J.-P. Boulanger, C. Menkes, P. Delecluse, P. Inness, J. Cole, and J. Slingo, 2004: Triggering of El Niño by westerly wind events in a coupled general circulation model. *Climate Dyn.*, **23**, 601–620.

Monahan, A. H., 2008: Probability distribution of sea surface wind stresses. *Geophys. Res. Lett.*, **35**, L05704, doi:doi:10.1029/2007GL032268.

Perez, C. L., A. M. Moore, J. Zavala-Garay, and R. Kleeman, 2005: A comparison of the influence of additive and multiplicative stochastic forcing on a coupled model of ENSO. *J. Climate*, **18**, 5066–5085.

Philip, S. Y. and G. J. van Oldenborgh, 2006: Shifts in ENSO coupling processes under global warming. *Geophys. Res. Lett.*, **33**, L11704, doi:doi:10.1029/2006GL026196.

Sura, P., M. Newman, and M. A. Alexander, 2006: Daily to decadal sea surface temperature variability driven by state-dependent stochastic heat fluxes. *J. Phys. Oceanogr.*, **36**, 1940–1958.

Sura, P., M. Newman, C. Penland, and P. D. Sardeshmukh, 2005: Multiplicative noise and non-gaussianity: A paradigm for atmospheric regimes? *J. Atmos. Sci.*, **62**, 1391– 1409.

Tziperman, E. and L. Yu, 2007: Quantifying the dependence of westerly wind bursts on the large scale tropical Pacific SST. *J. Climate*, **20**, 2760–2768.

Uppala, S. M., P. W. Kålberg, A. J. Simmons, U. Andrae, V. da Costa Bechtold, M. Fiorino, J. K. Gibson, J. Haseler, A. Hernandez, G. A. Kelly, X. Li, K. Onogi, S. Saarinen, N. Sokka, R. P. Allan, E. Anderson, K. Arpe, M. A. Balmaseda, A. C. M. Beljaars, L. van den Berg, J. Bidlot, N. Borman, S. Caires, A. Dethof, M. Dragosavac, M. Fisher, M. Fuentes, S. Hagemann, E. Hólm, B. J. Hoskins, L. Isaksen, P. A. E. M. Janssen, R. Jenne, A. P. McNally, J.-F. Mahfouf, J.-J. Mocrette, N. A. Rayner, R. W. Saunders, P. Simon, A. Sterl, K. E. Trenberth, A. Untch, D. Vasiljevic, P. Viterbo, and J. Woollen, 2005: The ERA-40 re-analysis. *Quart. J. Roy. Meteor. Soc.*, **130**, 2961–3012, doi:10.1256/qj.04.176.

van Oldenborgh, G. J., S. Y. Philip, and M. Collins, 2005: El Niño in a changing climate: a multi-model study. *Ocean Science*, **1**, 81–95.

Zebiak, S. E. and M. A. Cane, 1987: A model of El Niño–Southern Oscillation. *Mon. Wea. Rev.*, **115**, 2262–2278.

List of Figures

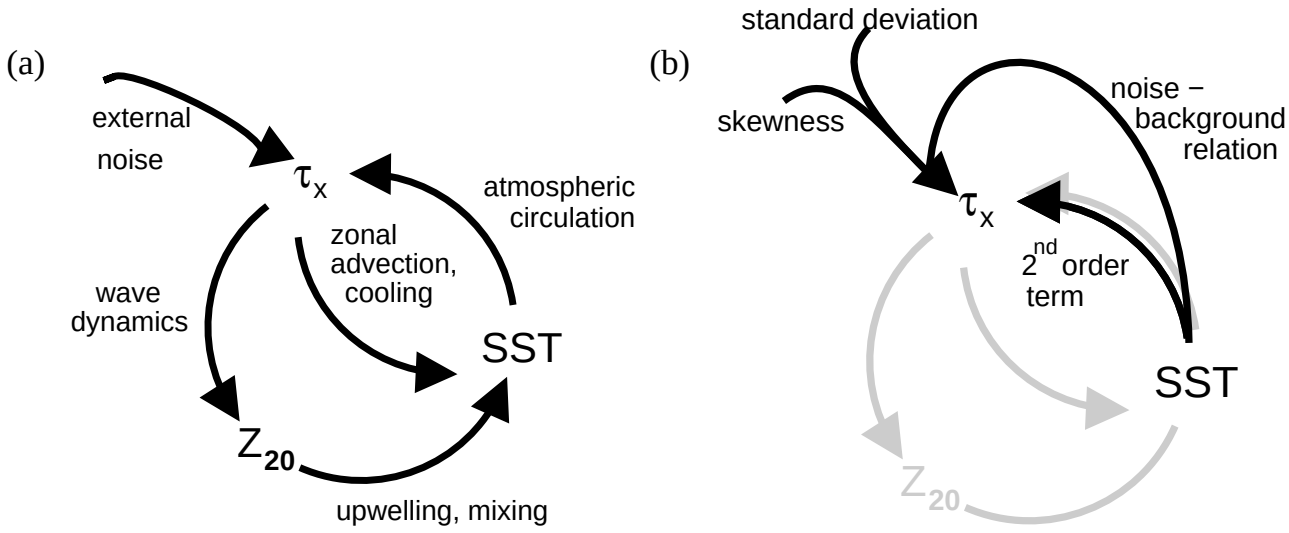

FIG. 1. The main feedbacks between wind stress (τ_x), SST and thermocline depth (Z_{20}) in the ENSO cycle and the driving external noise term. a) shows the linear feedbacks and b) shows the contribution of noise properties and nonlinear terms examined in this study.

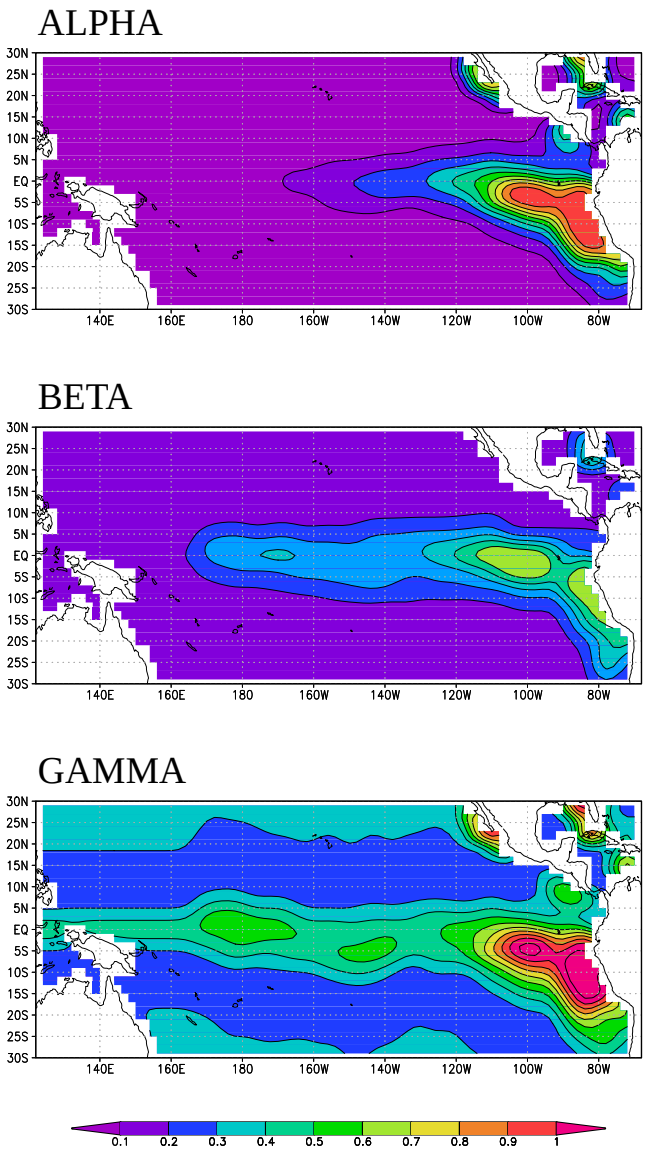

FIG. 2. 2-dimensional parameters as described in Equation 3, deduced from SODA data. α is the SST response to thermocline anomalies [$0.1\mathrm{Km}^{-1}\mathrm{month}^{-1}$], β is the SST response to wind variability [$100\mathrm{KPa}^{-1}\mathrm{month}^{-1}$] and γ is the damping [month^{-1}].

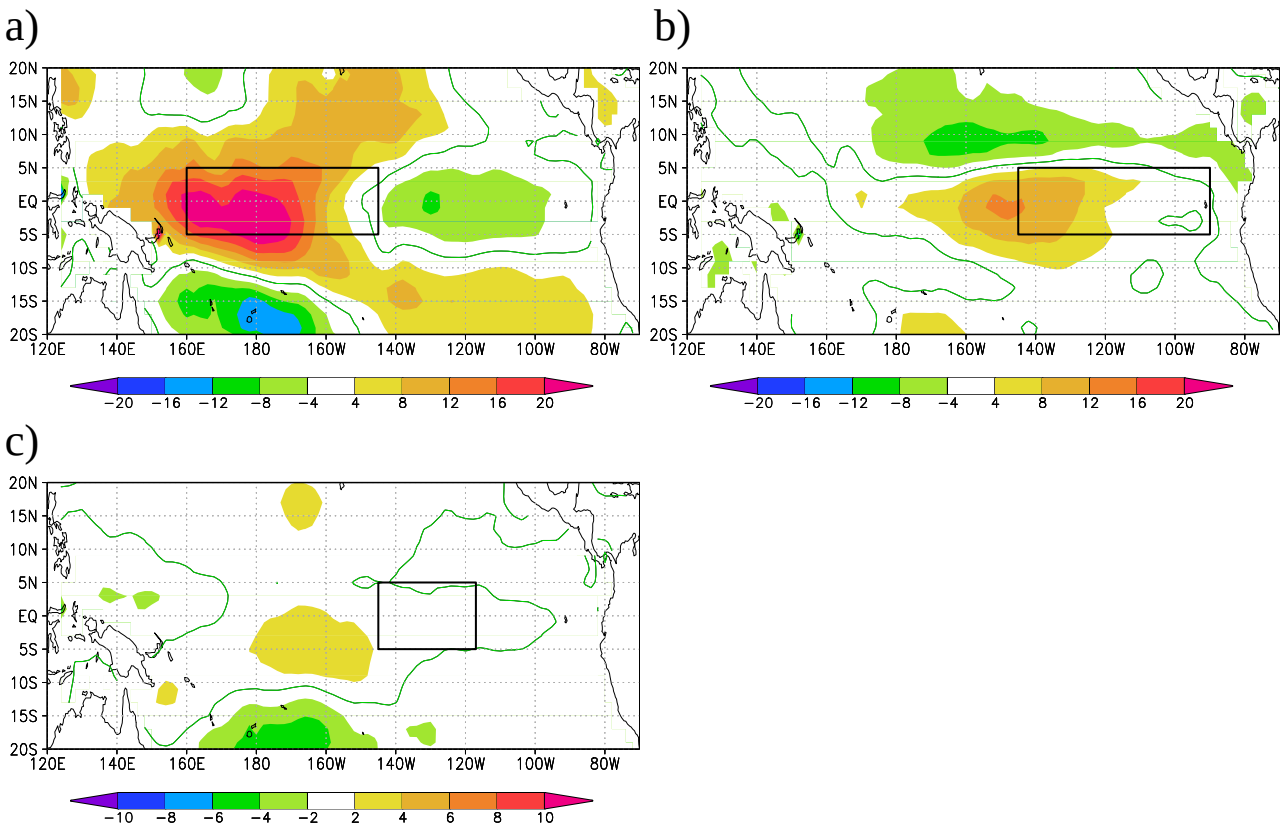

FIG. 3. Wind response $[10^{-3}\mathrm{Nm}^{-2}\mathrm{K}^{-1}]$ to an SST anomaly in the box only. a) linear wind response to an SST anomaly in the Niño4 region, b) linear wind response to an SST anomaly in the Niño3 region and c) quadratic wind response to an SST anomaly in the left half of the Niño3 region. Positive means a wind anomaly to the east, negative means a wind anomaly to the west. Note the difference in scale between the linear and nonlinear response.

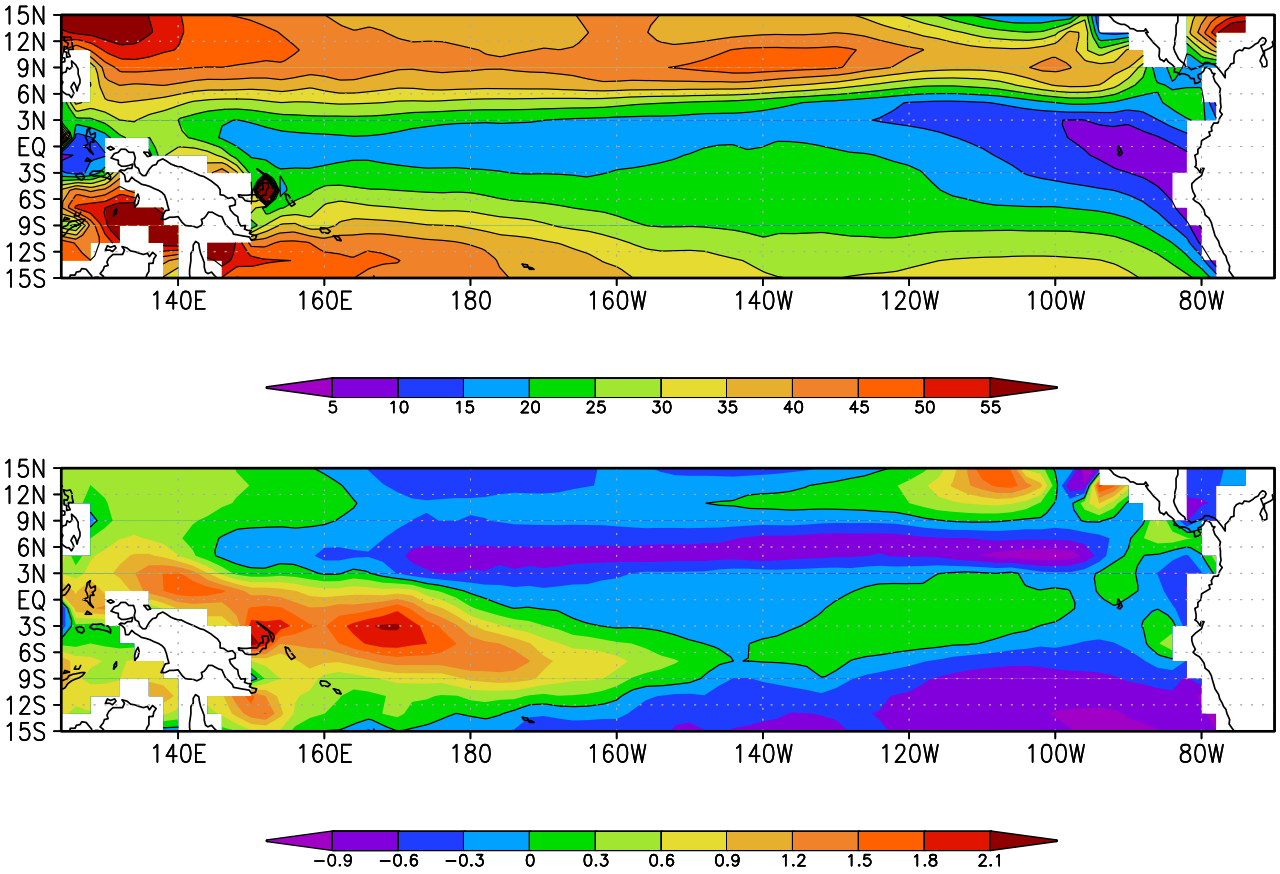

FIG. 4. Standard deviation $[10^{-3}\mathrm{Nm}^{-2}]$ (top) and skewness (bottom) of noise used to describe the nonlinear atmosphere. Positive skewness means stronger westerly than easterly anomalies.

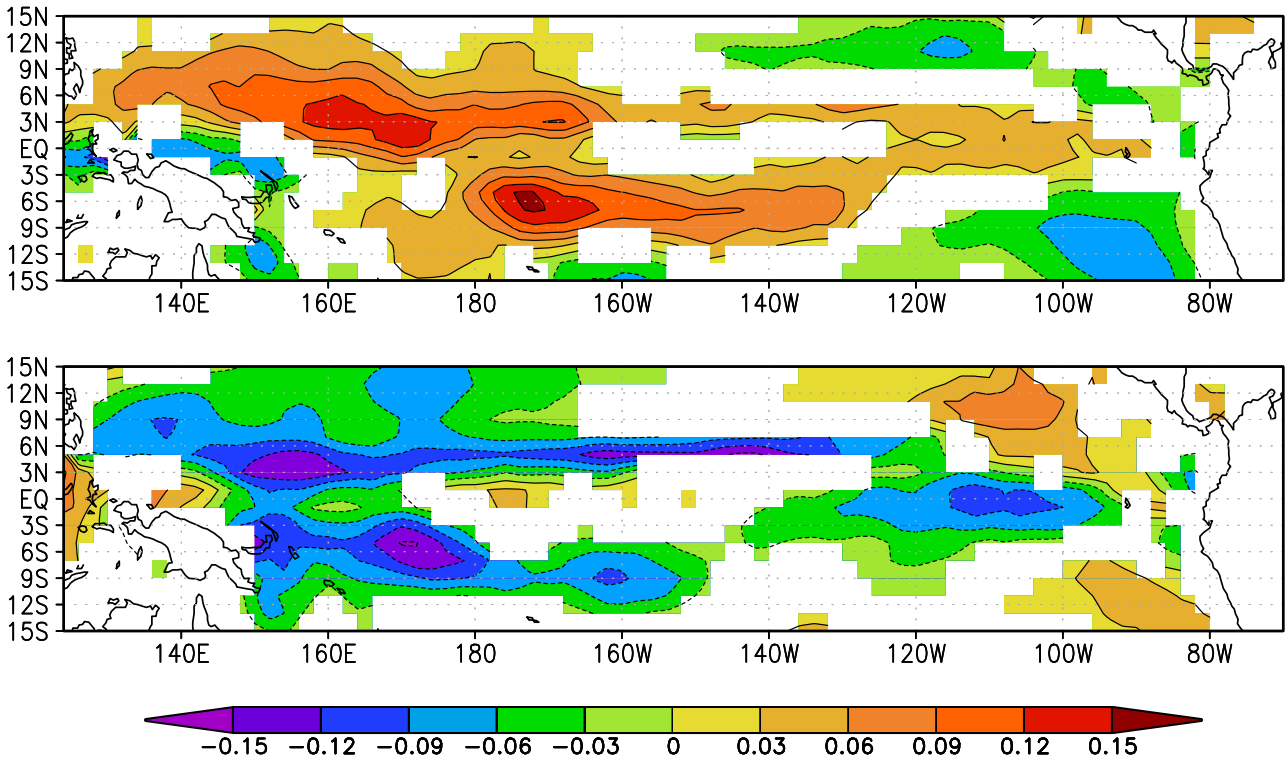

FIG. 5. Difference in standard deviation between the El Niño and neutral phase (top) and the La Niña and neutral phase (bottom) as $(\sigma_{\text{warm}} - \sigma_{\text{neutral}})/(\sigma_{\text{warm}} + \sigma_{\text{neutral}})$ and $(\sigma_{\text{cold}} - \sigma_{\text{neutral}})/(\sigma_{\text{cold}} + \sigma_{\text{neutral}})$, for noise used to describe the nonlinear atmosphere.

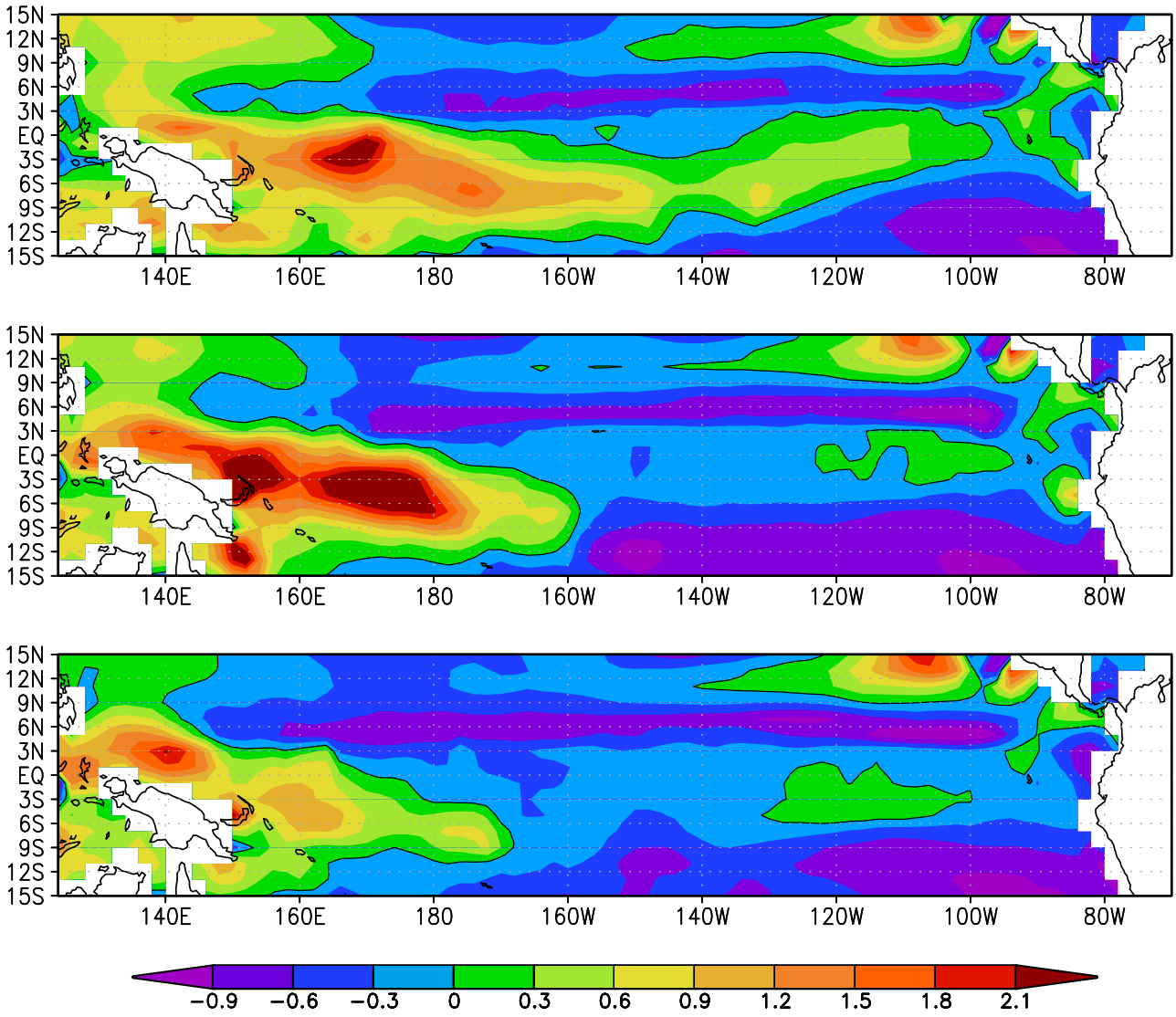

FIG. 6. Top to bottom: skewness of noise used to describe the nonlinear atmosphere for the warm, neutral and cold phase respectively.

EOF1

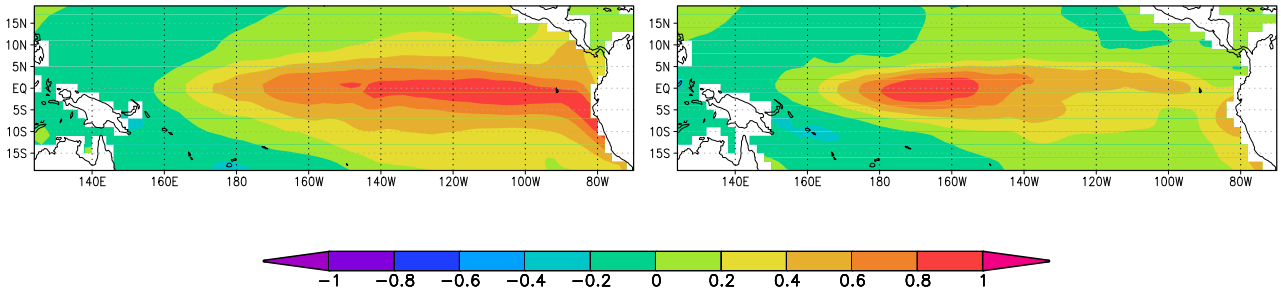

SPECTUM

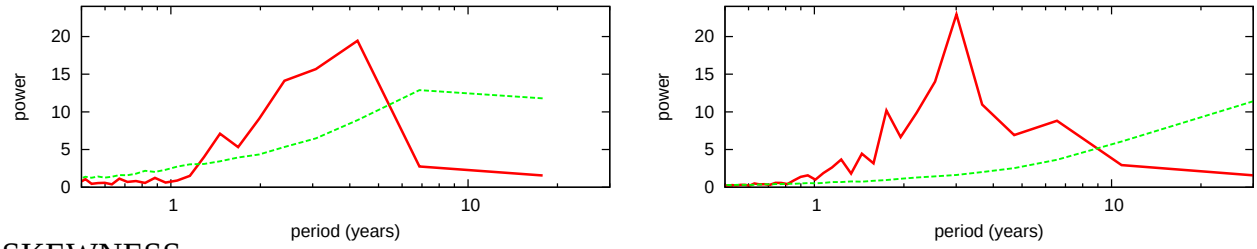

SKEWNESS

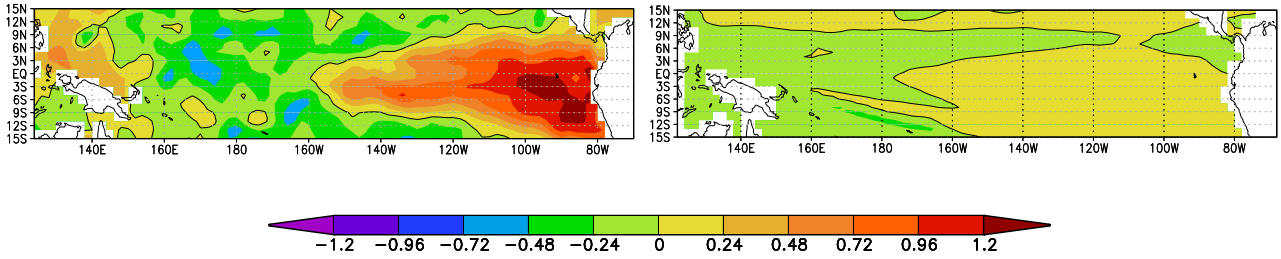

FIG. 7. First EOF, spectrum and skewness of SST of re-analysis (left) (Uppala et al. 2005) and of the linear ICM (right). Dashed lines in the spectrum figures denote the significance level.

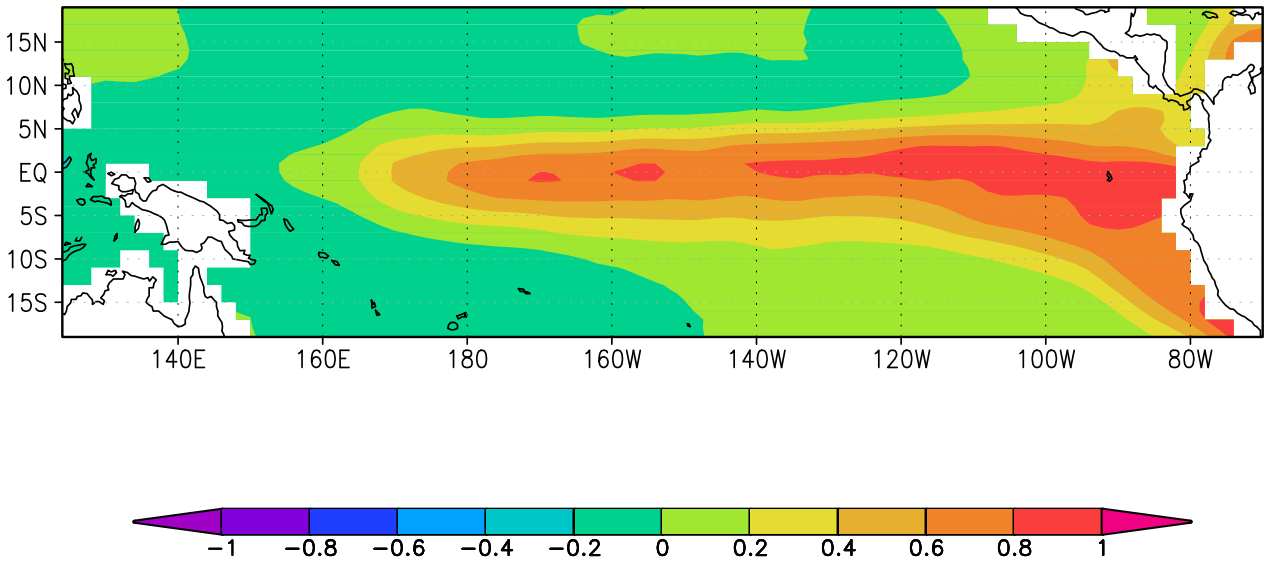

FIG. 8. First EOF of the ICM SST with linear atmosphere and 'full sd noise' which is ENSO-phase independent (*lin/full-sd/fix*-experiment).

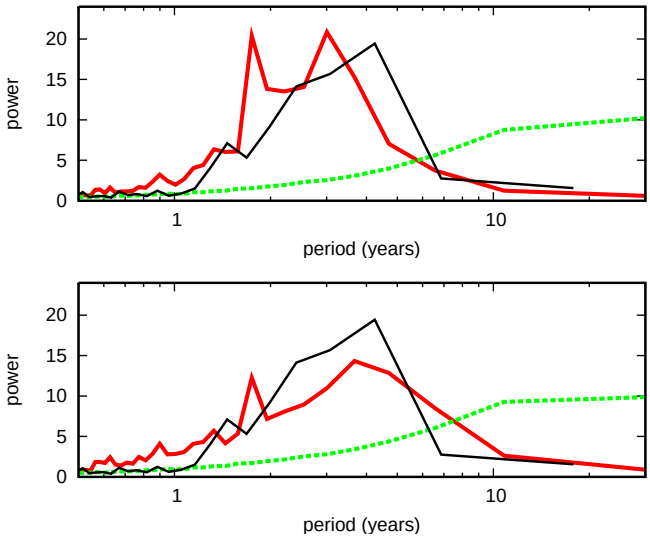

FIG. 9. Spectra of the ICM PC1 (thick lines) with linear atmosphere (top) and nonlinear atmosphere (bottom), both with 'full sd noise' which is ENSO-phase independent. The significance level of the period is given by the dashed lines. Thin lines show the spectrum of the ERA40 re-analysis.

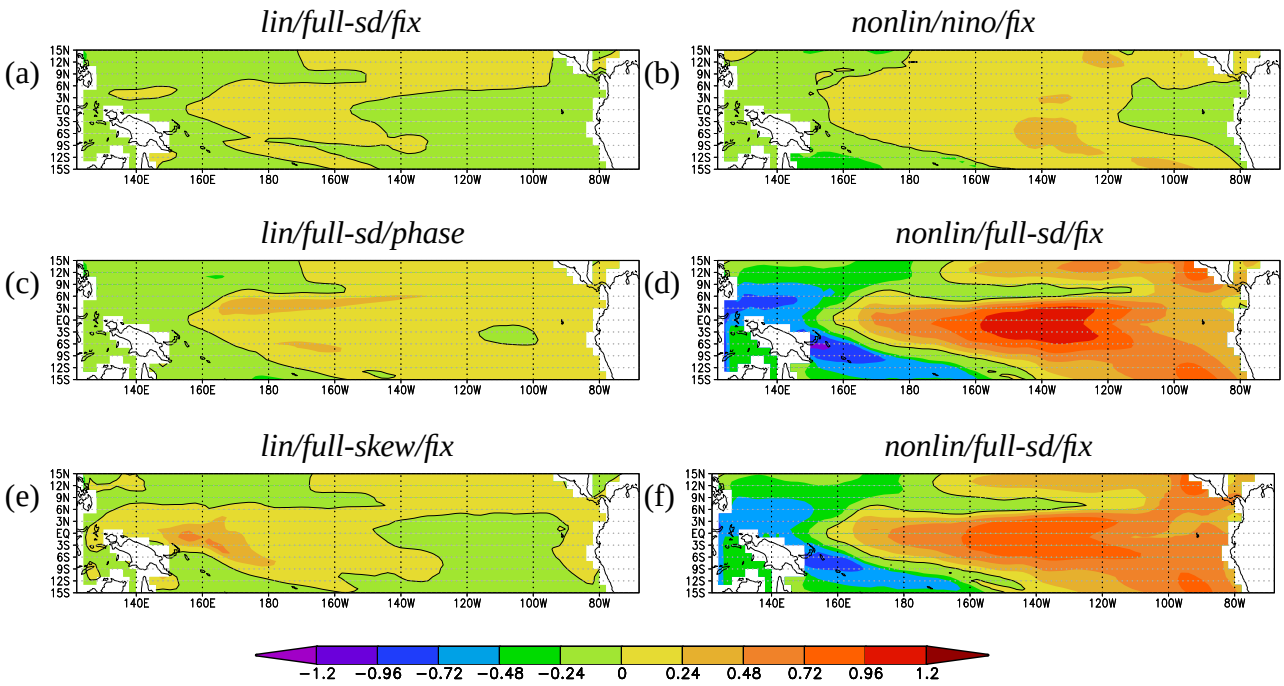

FIG. 10. Skewness of SST of the ICM for (a) linear atmosphere and fixed full noise standard deviation, (b) nonlinear atmosphere and noise on the SST indices, (c) linear atmosphere and full noise standard deviation dependent on the ENSO-phase, (d) nonlinear atmosphere and fixed full noise standard deviation, (e) linear atmosphere and full noise standard deviation and skewness dependent on the ENSO-phase and (f) nonlinear atmosphere and full noise standard deviation dependent on the ENSO-phase and bound on the thermocline(see Section 5).

List of Tables

TABLE 1. Different types of ICM experiments including abbreviations.

Characteristic	abbreviation	explanation
Statistical atmosphere	*lin*	linear statistical atmosphere (Equation 1)
	nonlin	nonlinear statistical atmosphere (Equation 2)
Noise	*nino*	red plus white noise on the SST anomalies
	full-sd	noise on the wind stress field with prescribed standard deviation, spatial correlations and time correlation
	full-skew	noise on the wind stress field with prescribed standard deviation, skewness, spatial correlations and time correlation
ENSO phase	*fix*	noise field is independent on the ENSO phase
	phase	noise depends on the ENSO phase, e.g., El Niño, neutral, La Niña